

Fabrication of photocatalyst panels and the factors determining their activity for water splitting†

Cite this: *Catal. Sci. Technol.*, 2014, 4, 325Received 25th October 2013,
Accepted 26th November 2013

DOI: 10.1039/c3cy00845b

www.rsc.org/catalysis

A photocatalyst panel of $\text{Rh}_{2-y}\text{Cr}_y\text{O}_3/(\text{Ga}_{1-x}\text{Zn}_x)(\text{N}_{1-x}\text{O}_x)$ exhibiting activity comparable to that of a conventional powder suspension system was developed by spreading the photocatalyst powder onto 5 cm × 5 cm flat frosted glass plates together with micrometer-sized hydrophilic silica particles, which improved the porosity of the photocatalyst layer for more efficient mass diffusion through the photocatalyst layer.

Due to global environmental problems caused by the mass use of fossil fuels as well as growing energy demands anticipated in the future, the development of a clean and renewable energy resource based on solar energy has been explored for a number of years. The conversion of solar energy to hydrogen *via* photocatalytic water splitting is a promising solution.^{1–5} Many photocatalysts that work under ultraviolet irradiation with excellent quantum efficiencies have been developed.^{4,6} In addition, overall water splitting under visible light has also been achieved in some oxynitrides.^{7–16}

In these previous studies, typically the photocatalyst powder was suspended in a reaction solution to ensure sufficient mass transfer. However, the use of photocatalyst suspensions has many difficulties in terms of dispersion, separation, and collection of the photocatalyst for large-scale applications.

Anke Xiong,^a Guijun Ma,^a Kazuhiko Maeda,^{‡ab} Tsuyoshi Takata,^{§a} Takashi Hisatomi,^a Tohru Setoyama,^c Jun Kubota^a and Kazunari Domen^{*a}

The fabrication of a photocatalyst panel, wherein the photocatalyst powder is fixed on a specific substrate, could solve these aforementioned problems and make it easier to exchange samples in practical operation. Additionally, a photocatalyst panel can track the sun easily so that sunlight is absorbed most effectively during the day. Economic analysis has suggested that a sun-tracking concentrator array has an advantage in cost compared to a fixed panel array.¹⁷ However, no attempt has been made to fabricate a photocatalyst panel for water splitting thus far. In the present study, the $\text{Rh}_{2-y}\text{Cr}_y\text{O}_3/(\text{Ga}_{1-x}\text{Zn}_x)(\text{N}_{1-x}\text{O}_x)$ photocatalyst was employed as a model photocatalyst for fabricating photocatalyst panels. Photocatalyst panels of $\text{Rh}_{2-y}\text{Cr}_y\text{O}_3/(\text{Ga}_{1-x}\text{Zn}_x)(\text{N}_{1-x}\text{O}_x)$ 5 cm × 5 cm in size, maintaining the inherent activity of the powder suspension, were developed through modification of the porosity and hydrophilicity of the photocatalyst panels by mixing silica of different sizes.

A $(\text{Ga}_{1-x}\text{Zn}_x)(\text{N}_{1-x}\text{O}_x)$ photocatalyst modified with the $\text{Rh}_{2-y}\text{Cr}_y\text{O}_3$ cocatalyst was prepared, as we have previously reported,¹⁵ and was used to fabricate photocatalyst panels using the squeegee and drop-casting methods. The squeegee method is a popular method to fix photocatalyst powder onto a substrate. In fact, GaN:ZnO photoelectrodes were prepared using this method in an earlier study.¹⁸ A slurry of the photocatalyst, acetylacetone, and a surfactant (Triton X) in distilled water was spread on a glass plate with a glass rod and then calcined at 673 K for 1 h for the squeegee method. On the other hand, a slurry of the photocatalyst mixed with silica powder, if necessary, in distilled water was dropped and dried at 323 K for the drop-cast method. All the photocatalyst panels were opaque because of scattering. Experimental details of these two methods are provided in the ESI.†

Fig. 1 shows SEM images of the photocatalyst panels of $\text{Rh}_{2-y}\text{Cr}_y\text{O}_3/(\text{Ga}_{1-x}\text{Zn}_x)(\text{N}_{1-x}\text{O}_x)$, the nanometer-sized silica, and micrometer-sized silica particles. The photocatalyst plates prepared using the squeegee and drop-casting methods without silica exhibited similar morphologies, as seen in Fig. 1A and B, respectively. The photocatalyst particles, 200–400 nm in size (Fig. 1E), were piled thickly and voids were observed among

^a Department of Chemical System Engineering, The University of Tokyo, 7-3-1 Hongo, Bunkyo-ku, Tokyo 113-8656, Japan. E-mail: domen@chemsys.t.u-tokyo.ac.jp

^b Precursory Research for Embryonic Science and Technology (PRESTO), Japan Science and Technology Agency (JST), 4-1-8 Honcho Kawaguchi, Saitama 332-0012, Japan

^c Mitsubishi Chemical Group Science and Technology Research Center, 1000 Kamoshida, Aoba, Yokohama 227-8502, Japan

† Electronic supplementary information (ESI) available: Experimental; time course of photocatalytic water splitting using photocatalyst panels and powder suspensions. See DOI: 10.1039/c3cy00845b

‡ Current affiliation: Department of Chemistry, Graduate School of Science and Engineering, Tokyo Institute of Technology, 2-12-1-NE-2, Ookayama, Meguro-ku, Tokyo 152-8550, Japan.

§ Current affiliation: Photochemical Energy Conversion Group, Solar Energy Conversion Field, GREEN, National Institute for Materials Science, 1-2-1 Sengen, Tsukuba, Ibaraki 305-0047, Japan.

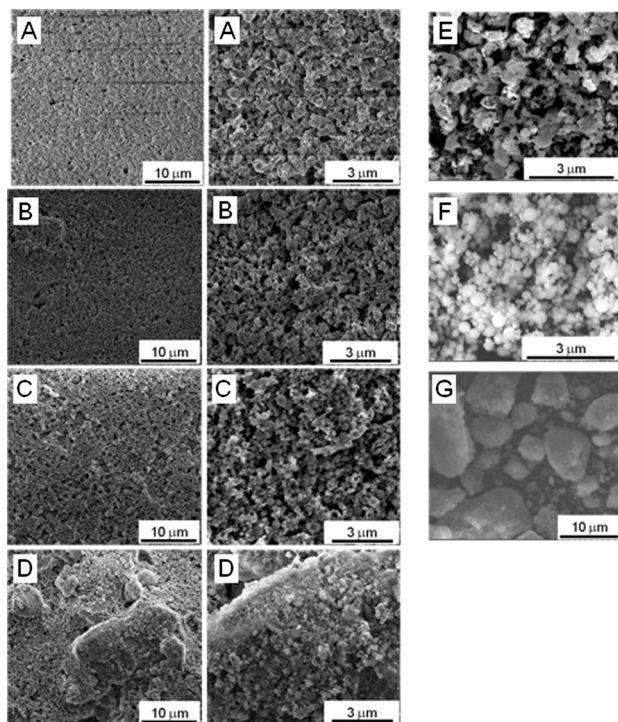


Fig. 1 SEM images of (A–D) $\text{Rh}_{2-y}\text{Cr}_y\text{O}_3/(\text{Ga}_{1-x}\text{Zn}_x)(\text{N}_{1-x}\text{O}_x)$ photocatalyst panels prepared using (A) the squeegee method, (B) the drop-casting method, (C) the drop-casting method with nanometer-sized SiO_2 , and (D) the drop-casting method with micrometer-sized SiO_2 . (E) $\text{Rh}_{2-y}\text{Cr}_y\text{O}_3/(\text{Ga}_{1-x}\text{Zn}_x)(\text{N}_{1-x}\text{O}_x)$ photocatalyst particles, (F) nanometer-sized SiO_2 particles, and (G) micrometer-sized SiO_2 particles.

the particles. The addition of SiO_2 particles to the photocatalyst suspension in the drop-cast method significantly changed the morphology of the photocatalyst panels. When nanometer-sized SiO_2 (Fig. 1F) was used, spherical nanometer-sized SiO_2 particles were located among comparatively larger photocatalyst particles (Fig. 1E), separating the photocatalyst particles from each other and creating small voids in the particle layer (Fig. 1C). On the other hand, the addition of micrometer-sized SiO_2 (Fig. 1G) resulted in a totally different morphology as shown in Fig. 1D. The micrometer-sized SiO_2 formed an uneven particle layer with large voids unlike in the other panel samples, and the larger SiO_2 particles appeared to be decorated with the photocatalyst particles.

The initial activity of the photocatalyst panels and powder for overall water splitting is summarized in Fig. 2. The photocatalyst panels prepared using the squeegee and drop-casting methods without silica particles split water to hydrogen and oxygen under UV light irradiation, as shown in Fig. 2A and B, respectively. The photocatalytic activity of the photocatalyst panel prepared using the drop-casting method exhibited three times higher activity than that prepared using the squeegee method. This is probably due to sintering of the photocatalyst layer caused by calcination in the squeegee method. However, the activities of the photocatalyst panels prepared without silica particles (Fig. 2A and B) were significantly lower than

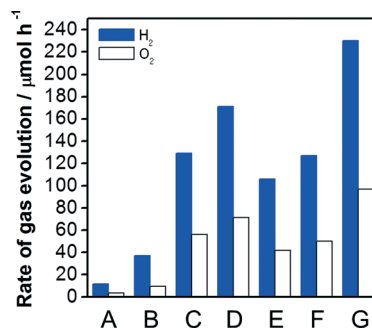


Fig. 2 Initial rates of photocatalytic water splitting on (A–D) the photocatalyst panels prepared using (A) the squeegee method, (B) the drop-casting method, (C) the drop-casting method with nanometer-sized SiO_2 , and (D) the drop-casting method with micrometer-sized SiO_2 . (E) Photocatalyst powder collected from the photocatalyst panel and precipitated on the bottom of the reactor, (F) fresh photocatalyst powder precipitated on the bottom of the reactor, and (G) the fresh photocatalyst powder suspension under stirring. Reaction conditions: photocatalyst powder, $\text{Rh}_{2-y}\text{Cr}_y\text{O}_3/(\text{Ga}_{1-x}\text{Zn}_x)(\text{N}_{1-x}\text{O}_x)$, 20 mg; SiO_2 , 20 mg; solution, H_2O 100 mL; light source, 300 W Xe lamp ($\lambda > 300$ nm); reaction vessel, Pyrex top-irradiation vessel. Filled and unfilled bars indicate H_2 and O_2 evolution rates, respectively.

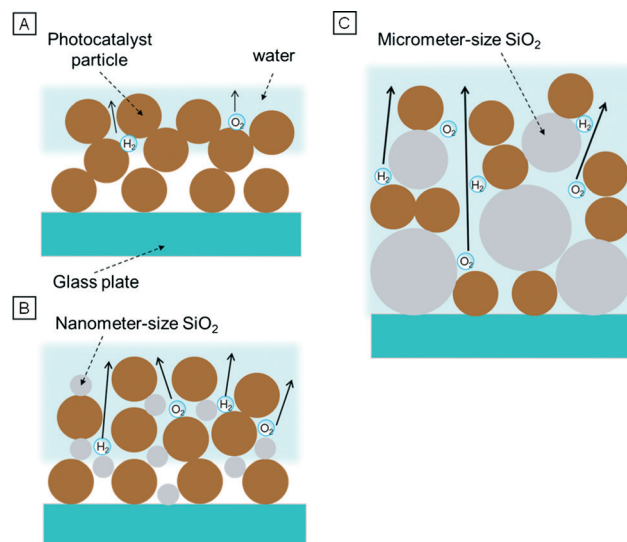
for the case where the same amount of photocatalyst powder precipitated on the bottom of the reactor was illuminated (Fig. 2F) despite the similar reaction conditions. This photocatalyst powder was collected *via* ultrasonication from the photocatalyst panel fabricated using the squeegee method after the reaction (Fig. 2A). The collected photocatalyst powder was suspended in a fresh reaction solution, precipitated at the bottom of the reactor, and illuminated for the additional reaction. The collected photocatalyst powder (Fig. 2E) showed almost the same activity as the fresh photocatalyst powder (Fig. 2F) when they were precipitated. This suggested that the preparation process of the photocatalyst panel using the squeegee method did not damage the photocatalyst particles. The low activity of the photocatalyst panels is likely due to the morphology of the photocatalyst layer which allowed only a part of the photocatalyst particles to contribute to photocatalytic water splitting.

To alter the morphology of the photocatalyst panel, $\text{Rh}_{2-y}\text{Cr}_y\text{O}_3/(\text{Ga}_{1-x}\text{Zn}_x)(\text{N}_{1-x}\text{O}_x)$ was mixed with different sized SiO_2 for fabricating the photocatalyst panels using the drop-casting method. The photocatalyst panel consisting of the photocatalyst and nanometer-sized SiO_2 particles (Fig. 2C) showed three times higher activity than the panel prepared without addition of SiO_2 (Fig. 2B); the former was comparable to the activity of the photocatalyst powder precipitated at the bottom of the reaction vessel (Fig. 2F). Presumably, inter-particle voids created by hydrophilic SiO_2 particles facilitated transport of water and evolved gases. In addition, the addition of SiO_2 improved the activity of the photocatalyst panel of Zn-doped Ga_2O_3 for water splitting (Fig. S1†) and that of the Mg-doped BaTaO_2N for the H_2 and O_2 evolution reactions from aqueous solutions of MeOH and AgNO_3 (Fig. S2 and S3†), respectively. Note that the effect of SiO_2 addition was more significant for Mg-doped BaTaO_2N than for Zn-doped Ga_2O_3 ,



because Mg-doped BaTaO₂N and GaN:ZnO were seemingly less hydrophilic than Zn-doped Ga₂O₃. These results clearly indicate the generally positive effect of incorporating SiO₂ particles into the photocatalyst powder on the morphology of the photocatalyst layers. However, increasing the amount of SiO₂ did not lead to further improvements in the photocatalytic activity of the photocatalyst panel (Fig. S4†). When micrometer-sized SiO₂ particles larger than the photocatalyst particles were applied, the activity of the photocatalyst panel was further enhanced (Fig. 2D). The reaction time course, shown in Fig. 3, indicated that the activities of these two systems were comparable although the initial activity of the photocatalyst panel was somewhat lower than that of the powder suspension under stirring (Fig. 2G).

The results of the photocatalytic reactions and SEM observations of the photocatalyst panels suggest that the photocatalytic activity becomes higher as the size of the voids in the photocatalyst particle layer becomes larger. This is explained on the basis of Scheme 1. When no SiO₂ is added, water does not penetrate into the thick photocatalyst particle layer, which does not have large voids. Therefore, the water would not be able to react with photocatalyst particles inside the photocatalyst particle layer. In addition, small voids would be easily blocked by bubbles of the evolved hydrogen and oxygen. Thus, only photocatalyst particles near the outer surface of the photocatalyst panel would react with water effectively under light illumination, yielding low photocatalytic activity. On the other hand, the addition of SiO₂ created many voids in the photocatalyst panels and offered more space for transfer of water and evolved gases through the photocatalyst particle layer. The addition of SiO₂ particles significantly larger than the photocatalyst particles was found to be more effective in providing interparticle voids for mass transfer. The hydrophilic nature of SiO₂ could also facilitate penetration of water through the photocatalyst particle layer.



Scheme 1 Illustrations of photocatalyst panels prepared (A) without SiO₂, (B) with nanometer-sized SiO₂, and (C) with micrometer-sized SiO₂. Brown and gray particles indicate secondary particles of (Ga_{1-x}Zn_x)(N_{1-x}O_x) and SiO₂, respectively.

The activity of the photocatalyst panel and suspension was found to decrease during the reaction (Fig. 3). This is due to hydrolysis of the (Ga_{1-x}Zn_x)(N_{1-x}O_x) photocatalyst in the neutral pH range.¹¹ By adjusting the pH of the reaction solution using H₂SO₄, the photocatalyst suspension system showed a stable reaction rate, as reported previously.¹¹ However, the pH of the reaction solution did not influence the durability of the photocatalyst panel significantly (Fig. S5†). This may be due to a change in local pH inside the photocatalyst particle layer because mass transfer is not promoted by convection. A technique to control the microscopic reaction conditions of the photocatalyst particle layers is needed for fabricating more durable photocatalyst panels.

Conclusions

In conclusion, photocatalyst panels of Rh_{2-y}Cr_yO₃/(Ga_{1-x}Zn_x)(N_{1-x}O_x) exhibiting high photocatalytic activity were developed by fixing the photocatalyst powder mixed with micrometer-sized SiO₂ powder onto 5 cm × 5 cm flat frosted glass plates. It was suggested that access for water inside the photocatalyst particle layer greatly influenced the activity of the photocatalyst panel. The porosity of the photocatalyst layer was crucial for access of water and for the release of the evolved gases. Adding SiO₂ created porosity suitable for mass transfer. The addition of micrometer-sized SiO₂ was found to be the most effective fabrication method for the photocatalyst panels. The activity of the photocatalyst panels containing micrometer-sized SiO₂ was comparable to that of the photocatalyst powder suspension. The fabrication process of the photocatalyst panel, involving inexpensive SiO₂ powder as an additive, is simple and is applicable to various photocatalysts and substrates, including flexible plastic sheets, on a large-scale.

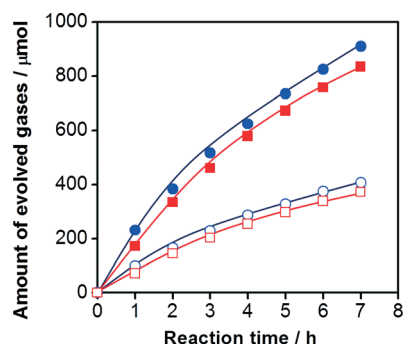


Fig. 3 Time courses of photocatalytic water splitting using the photocatalyst panel and powder. Reaction conditions: photocatalyst powder, Rh_{2-y}Cr_yO₃/(Ga_{1-x}Zn_x)(N_{1-x}O_x), 20 mg; SiO₂, 20 mg; solution, H₂O 100 mL; light source, 300 W Xe lamp ($\lambda > 300$ nm); reaction vessel, Pyrex top-irradiation vessel. Rectangles and circles represent data for the photocatalyst panels prepared using the drop-casting method with micrometer sized SiO₂ and the photocatalyst suspension system, respectively. Closed and open symbols denote H₂ and O₂, respectively.



The developments and results of this study are anticipated to promote the use of photocatalytic solar water splitting for versatile and practical applications.

Acknowledgements

This work was supported in part by a Grant-in-Aid for Specially Promoted Research (#23000009) of the Japan Society for the Promotion of Science (JSPS) and the Advanced Low Carbon Technology Research and Development Program (ALCA) of the Japan Science and Technology Agency (JST). This work was also partly supported by the Funding Program for World-Leading Innovative R&D in Science and Technology (FIRST) of the Cabinet Office of Japan. This work also contributes to the international exchange program of the A3 Foresight Program of JSPS. One of the authors (A.X.) was supported by the Japan Chemical Industry Association. One of the authors (K.M.) thanks the Nippon Sheet Glass Foundation for Materials Science and Engineering for funding support.

Notes and references

- 1 J. S. Lee, *Catal. Surv. Asia*, 2005, **9**, 217.
- 2 K. Maeda and K. Domen, *J. Phys. Chem. C*, 2007, **111**, 7851.
- 3 F. E. Osterloh, *Chem. Mater.*, 2008, **20**, 35.
- 4 A. Kudo and Y. Miseki, *Chem. Soc. Rev.*, 2009, **38**, 253.
- 5 K. Maeda and K. Domen, *J. Phys. Chem. Lett.*, 2010, **1**, 2655.
- 6 H. Kato, K. Asakura and A. Kudo, *J. Am. Chem. Soc.*, 2003, **125**, 3802.
- 7 K. Maeda, T. Takata, M. Hara, N. Saito, Y. Inoue, H. Kobayashi and K. Domen, *J. Am. Chem. Soc.*, 2005, **127**, 8286.
- 8 K. Maeda, K. Teramura, T. Takata, M. Hara, N. Saito, K. Toda, Y. Inoue, H. Kobayashi and K. Domen, *J. Phys. Chem. B*, 2005, **109**, 20504.
- 9 K. Teramura, K. Maeda, T. Saito, T. Takata, N. Saito, Y. Inoue and K. Domen, *J. Phys. Chem. B*, 2005, **109**, 21915.
- 10 K. Maeda, K. Teramura, D. Lu, T. Takata, N. Saito, Y. Inoue and K. Domen, *Nature*, 2006, **440**, 295.
- 11 K. Maeda, K. Teramura, H. Masuda, T. Takata, N. Saito, Y. Inoue and K. Domen, *J. Phys. Chem. B*, 2006, **110**, 13107.
- 12 K. Maeda, K. Teramura, D. Lu, T. Takata, N. Saito, Y. Inoue and K. Domen, *J. Phys. Chem. B*, 2006, **110**, 13753.
- 13 K. Maeda, K. Teramura, N. Saito, Y. Inoue and K. Domen, *J. Catal.*, 2006, **243**, 303.
- 14 K. Maeda, K. Teramura, D. Lu, N. Saito, Y. Inoue and K. Domen, *Angew. Chem., Int. Ed.*, 2006, **45**, 7806.
- 15 K. Maeda, K. Teramura and K. Domen, *J. Catal.*, 2008, **254**, 198.
- 16 K. Sayama, K. Mukasa, R. Abe, Y. Abe and H. Arakawa, *Chem. Commun.*, 2001, 2416.
- 17 B. Pinaud, J. Benck, L. Seitz, A. Forman, Z. Chen, T. Deutsch, B. James, K. Baum, G. Baum, S. Ardo, H. Wang, E. Miller and T. Jaramillo, *Energy Environ. Sci.*, 2013, **6**, 1983.
- 18 H. Hashiguchi, K. Maeda, R. Abe, A. Ishikawa, J. Kubota and K. Domen, *Bull. Chem. Soc. Jpn.*, 2009, **82**, 401.

